A Journal of the Gesellschaft Deutscher Chemiker
Angewandte Chemie
GDCh
International Edition
www.angewandte.org

Accepted Article

Title: A Versatile Metalloporphyrinic Framework Platform for Highly Efficient Bioinspired, Photo and Asymmetric Catalysis

Authors: Chuan-De Wu, Wei-Long He, and Min Zhao

To be cited as: *Angew. Chem. Int. Ed.* 10.1002/anie.201810294
Angew. Chem. 10.1002/ange.201810294

Link to VoR: http://dx.doi.org/10.1002/anie.201810294
http://dx.doi.org/10.1002/ange.201810294

WILEY-VCH

A Versatile Metalloporphyrinic Framework Platform for Highly Efficient Bioinspired, Photo and Asymmetric Catalysis

Wei-Long He,[a] Min Zhao,[a] and Chuan-De Wu*[a]

Dedicated to Professor Jin-Shun Huang on the occasion of his 80th birthday

Abstract: Even though numerous bioinspired catalysts have been developed, there remain huge gaps between the artificial and natural catalysts, because it is very difficult to imitate simultaneously the complicated constituents, structures and synergistic effect of enzymes. We report herein a versatile metalloporphyrinic framework platform, which exhibits high efficiency in bioinspired catalysis, photocatalysis and asymmetric catalysis. The catalytic properties are highly depending on the tunable constituents and their cooperation work, which are significantly superior to the corresponding molecular catalyst systems due to lack of synergistic work. Since there have been numerous functional moieties that are readily being incorporated into the platform, a myriad of applications can be therefore simply realized by imbedding different functional moieties.

Enzymes are a family of intriguing biocatalysts, which are very powerful in numerous catalytic reactions.[1] To imitate the catalytic properties of enzymes, numerous bioinspired catalysts, similar to the structures of redox-active centers of enzymes, have been therefore created.[2] However, because the constituents and structures of biocatalysts are very complicated, and biocatalysis is the synergistic work of multiple factors, the catalytic properties of bioinspired catalysts remain much inferior to those of the native enzymes.[3,4] The challenge to realize highly efficient bioinspired catalysis is how to imitate the catalytic mechanisms of enzymes for synergistic catalysis by exactly tuning the constituents, structures and locations of active sites in catalysts.

Metal-organic frameworks (MOFs) are an emerging class of porous materials constructed from multidentate organic ligands and metal ions/clusters, featuring high porosity, high surface areas, and tunable pore sizes and shapes.[5-12] The tunable pore nature and constituents of MOFs endow systematically introduce different redox-active and auxiliary centers to improve the catalytic properties.[13-23] MOFs represent a very promising class of porous materials for bioinspired catalysis.[3,4] However, the catalytic properties of bioinspired MOFs remain much inferior to those of the native enzymes, due to lack of systematically tunable MOF platform.[21-23] We report herein a porous metalloporphyrinic framework platform, $[Y_3(H_2O)_4(M\text{-}\mathbf{L})(CH_3COO)]\cdot$solvent (CZJ-18(M); M = $2H^{I}$, $Mn^{III}Cl$ and Cu^{II}; $H_{10}\mathbf{L}$ = 5,10,15,20-tetrakis-3,5-bis((4-hydroxycarbonyl)-phenyl)phenylporphine; Scheme S1), which is systematically modifiable with different functional moieties to tune the catalytic properties. In the structures of CZJ-18(M), not only the porphyrin metal centers are systematically tunable, but also the in situ imbedded acetate moieties in the frameworks are exchangeable with different functional moieties for highly efficient bioinspired catalysis, photocatalysis and asymmetric catalysis.

Brownish crystals of metalloporpyrinic frameworks CZJ-18(M) were synthesized by heating a mixture of M-H_8**L** and $Y(NO_3)_3\cdot 6H_2O$ in a mixed solvent of DMF and acetic acid at 80 °C for one week. These isostructural metalloporpyrinic frameworks are built from trigonal $[Y_3(H_2O)_4(\text{benzoate})_8(\text{acetate})]$ (abbreviated as $\{Y_3\}$) secondary building units (SBUs) and octatopic M-**L** linkers. In the crystal structures, each deprotonated M-**L** linker connects with eight trigonal $\{Y_3\}$ SBUs, and each $\{Y_3\}$ SBU connects with eight M-**L** linkers to form 3D non-interpenetrated networks with pore dimensions of about 1.8 nm (Figure 1a).

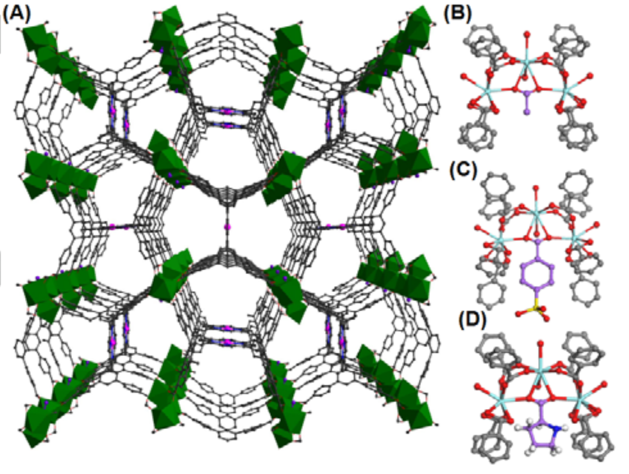

Figure 1. (A) The crystal structure of CZJ-18(Cu), consisting of accessible porphyrin Cu^{II} sites (pink balls). (B) The structure of $[Y_3(H_2O)_4(\text{benzoate})_8(\text{acetate})]$ in CZJ-18(Cu), highlighting the replaceable acetate moiety. (C) The simulated structure of $[Y_3(H_2O)_4(\text{benzoate})_8(\text{SB})]$ in CZJ-18(Cu)-SB. (D) The simulated structure of $[Y_3(H_2O)_4(\text{benzoate})_8(\text{Pro})]$ in CZJ-18(Cu)-Pro. Color scheme: Cu, pink balls; Y, green polyhedra and cyan balls; O, red; N, blue; C, deep gray and purple; S, yellow.

According to the coordination environments of Y^{III} ions, there are two kinds of Y^{III} ions in $[Y_3(H_2O)_4(\text{benzoate})_8(\text{acetate})]$ (Figure 1b). The acetate moiety acts as an η^4-ligand to bridge firmly three Y^{III} ions, playing very important roles to stabilize and neutralize the framework structures of CZJ-18(M), which is very difficult to be exchanged by post-modification. It is interesting that acetate is systematically replaceable with different functional moieties consisting of carboxylate groups to tune the catalytic properties by in situ assembly strategy. When 4-sulfobenzoate (SB) and L-proline (Pro) were used instead of

---

[a] W.-L. He, M. Zhao and Prof. Dr. C.-D. Wu
State Key Laboratory of Silicon Materials
Department of Chemistry
Zhejiang University
Hangzhou, 310027, P. R. China
E-mail: cdwu@zju.edu.cn

Supporting information for this article is given via a link at the end of the document.

10.1002/anie.201810294

acetic acid during synthesis of CZJ-18(M), these moieties were readily incorporated into the platform to form CZJ-18(Cu)-SB and CZJ-18(Cu)-Pro, respectively (Figure 1c and 1d). The strong attachment of different functional moieties to $\{Y_3\}$ clusters in CZJ-18(M) would ensure their stability during catalysis.

CZJ-18(Cu), CZJ-18(Cu)-SB and CZJ-18(Cu)-Pro take up 948, 503 and 434 $cm^3\ g^{-1}$ N_2 at 77 K and 1 bar, resulting microporous BET surface areas of 701.1, 386.1 and 490.5 m^2/g, respectively. The average pore widths are of about 1.8 nm, which are consistent well with the single crystal structures. Such high surface areas provide enough void space to accommodate and exchange further with different guest molecules. We selected CZJ-18(Cu) as a representative example to study the accessibility of the inside pores to different solvent molecules. GC results showed that CZJ-18(Cu) can readily take up large amounts of different solvent molecules, including acetonitrile, ethanol, acetone, toluene, tetrahydrofuran, styrene, styrene oxide, benzyl alcohol, benzaldehyde and cyclohexanone (Figure S34). Apparently, the inside pore space of CZJ-18(Cu) is readily accessible to small organic molecules transferred through the open channels, which would facilitate highly efficient catalysis.

To evaluate the accessibility of the porphyrin metal sites in CZJ-18(M), we examined the catalytic properties of CZJ-18(Mn) for epoxidation of olefins at room temperature. When a mixture of styrene substrate, iodosylbenzene (PhIO) oxidant and CZJ-18(Mn) catalyst in CH_3CN was stirred at room temperature for 19 h, GC-MS analysis showed that styrene was almost fully oxidized with 99% selectivity for the epoxide product (Table S2). CZJ-18(Mn) is much superior to the homogeneous molecular counterpart $Mn^{III}Cl$-Me_8OCPP in terms of substrate conversion (40%) and epoxide product selectivity (74%). CZJ-18(Mn) also epoxidized a series of olefins under the identical conditions. Accompanying increase of the substrate size, the conversion decreases gradually, because the bulky substrates have difficulty to access the active sites inside the pores of CZJ-18(Mn). CZJ-18(Mn) is very stable, which can be simply recovered and reused for six cycles with almost retained high catalytic efficiency. In contrast, the recovered molecular catalyst MnCl-Me_8OCPP did not active after the second cycle. These results indicate that incorporation of molecular bioinspired catalysts into the platform would significantly improve the catalytic efficiency and stability.

We have demonstrated that suspending redox-active metal ions in the anionic pores of MOFs would endow almost full available of the coordination sites of redox-active metal centers, which results in most dangling bonds and empty *d* atomic orbitals to maximize the catalytic efficiency.[24] It is interesting that the electronic charge of CZJ-18(M) is systematically tunable with differently charged moieties. When 4-sulfobenzoate was used instead of acetic acid during synthesis of these porous materials, the anionic moieties were successfully incorporated into the frameworks to form anionic CZJ-18(M)-SB. Treatment of CZJ-18(Cu)-SB with a DMF solution of copper(II) perchlorate resulted in a suspended ion catalyst (SIC) CZJ-18(Cu)-Cu, in which the extra-framework counter ions were almost fully exchanged by Cu^{II} ions as confirmed by ICP-MS and EDX spectroscopy.

Compared with those of $Cu(ClO_4)_2$, the binding energies of porphyrin Cu^{II} $2p_{3/2}$ and $2p_{1/2}$ in CZJ-18(Cu)-SB are significantly negative-shifted, because the binding energies are highly sensitive to the coordination environment (Figure S39).[25] It is interesting that the binding energies of suspended Cu^{II} ions in CZJ-18(Zn)-Cu are similar to those of porphyrin Cu^{II} in CZJ-18(Cu)-SB. These results indicate that the suspended Cu^{2+} and porphyrin Cu^{II} have similar electronic coordination environments. As expected, the differences of the binding energies for porphyrin and suspended Cu^{II} in CZJ-18(Cu)-Cu are negligible with the Cu $2p_{3/2}$ signal centered at 934.5 eV. The EPR signals of CZJ-18(Zn)-Cu are also different from those of $Cu(ClO_4)_2$. Similar to the XPS results, CZJ-18(Cu)-Cu, consisting of both porphyrin and suspended Cu^{II}, exhibits merged EPR signals (Figure S40). Compared with our previous results, the above results indicate that Cu^{II} ions should be suspended in the anionic pores with highly vacant coordination sphere by weakly attached to the pore surfaces, which are freely mobile in the negative-charged pore microenvironment for highly efficient catalysis.[24] N_2 adsorption experiments resulted in a BET surface area of 342.6 $m^2\ g^{-1}$ with the average pore width of 1.8 nm, which proved that suspending redox-active metal ions in the anionic pores does not significantly affect the porosity for highly efficient catalysis.

Considering that copper ions are the active sites of many redox enzymes, CZJ-18(Cu)-Cu was used as a bioinspired catalyst for aerobic oxidation of alcohols.[26,27] CZJ-18(Cu)-Cu is highly active in aerobic oxidation of alcohols in acetonitrile at 65 °C under 1 atm O_2 atmosphere (Figure 2 and Table S3). CZJ-18(Cu)-Cu efficiently prompted aerobic oxidation of benzyl alcohol with high yield of benzaldehyde (>99%). It is significantly superior to CZJ-18(Cu)-SB and CZJ-18(Cu), and molecular Cu-Me_8OCPP, which are almost inactive in the aerobic oxidation reaction. CZJ-18(Cu)-Cu is also much superior to a mixture of Cu-Me_8OCPP and copper perchlorate under the identical conditions (8.5%). These results demonstrate that suspending redox-active Cu^{II} ions in the anionic pores of CZJ-18(Cu)-Cu would significantly improve the catalytic activity by eliminating ligation of counter ions to the active sites, and letting catalytic reaction occur between Cu^{II} ions and framework anions to polarize and activate further the reactant molecules.

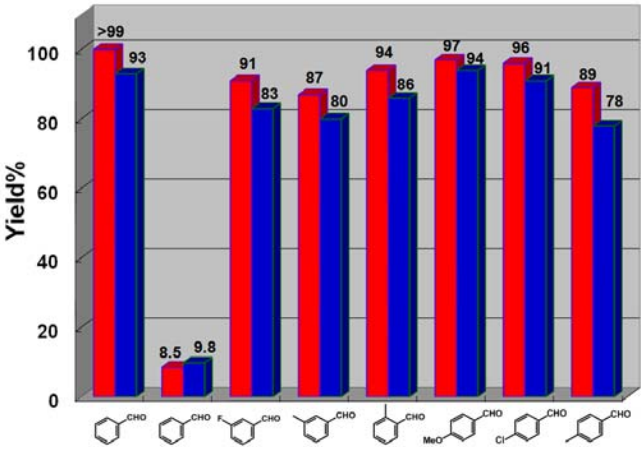

Figure 2. The yields of aldehydes catalyzed by CZJ-18(Cu)-Cu at 65 °C for 16 h (red columns) and CZJ-18(Zn)-Cu at room temperature for 10 h irradiated by visible light (blue columns). The numbers on the top of the columns are the yields of aldehydes. The third and fourth columns are the results catalyzed by Cu-$Me_8OCPP/Cu(ClO_4)_2$ and Zn-$Me_8OCPP/Cu(ClO_4)_2$, respectively.

CZJ-18(Cu)-Cu exhibited unique property for selective accumulation of substrate and release of product molecules. When the conversion of benzyl alcohol reached to 56%, about 0.37 wt% benzyl alcohol and 0.12 wt% benzaldehyde were detected from the collected solid catalyst. Moreover, when an activated sample of CZJ-18(Cu)-Cu was immersed in mixed benzyl alcohol and benzaldehyde (1:1 molar ratio) acetonitrile solution at room temperature, it took up benzyl alcohol (1.3 wt%) over benzaldehyde (0.44 wt%). These solid experimental results confirmed the preferred sorption capability of CZJ-18(Cu)-Cu for reactant molecules, which would significantly improve the catalytic efficiency and reaction rate. CZJ-18(Cu)-Cu can be reused for six cycles with almost retained high catalytic efficiency. ICP-MS analysis revealed that the suspended copper species did not leach into the supernate, which demonstrated that confining copper cations in the negative-charged pores by strong electrostatic interaction would prevent the leaching of copper ions. PXRD pattern of the recovered solid is almost identical to that of the as-synthesized one, which proved the structural integrity of CZJ-18(Cu)-Cu during catalysis. CZJ-18(Cu)-Cu is also highly efficient for selective aerobic oxidation of a range of alcohols to afford valuable aldehydes under the identical conditions. The turnover number reached to 17560 with an average turnover frequency of 251 h^{-1} (Figure S41).

Even though the metalloporphyrin moieties in CZJ-18(M)-Cu are almost inactive in the aerobic oxidation, however, they might act as effective photosensitizers to absorb visible light for the activation of O_2 oxidant, which would endow the aerobic oxidation reaction occur at room temperature.[28] It is interesting that CZJ-18(Zn)-Cu, consisting of $\mathrm{Zn^{II}}$-porphyrins as photosensitizers, efficiently prompted the aerobic oxidation reaction with high yield and selectivity for benzaldehyde product under visible light irradiation (Figure 2 and Table S4). Without SIC copper site in the anionic pores, CZJ-18(Zn)-SB is almost inactive in the aerobic oxidation reaction. These results demonstrated that $\mathrm{Zn^{II}}$-porphyrin is the efficient photosensitizer, SIC $\mathrm{Cu^{II}}$ is the excellent redox-active center, and the photocatalysis is the synergistic work of different active centers. The catalytic properties of CZJ-18(Zn)-Cu are significantly superior to those of the homogeneous mixture of Zn-$\mathrm{Me_8}$**L**/$\mathrm{Cu(ClO_4)_2}$ under the identical conditions. The improved photocatalytic oxidation efficiency of CZJ-18(Zn)-Cu should be attributed to incorporation of different active species in the pore space/matrix that endow them easily cooperative work.[29] CZJ-18(Zn)-Cu further demonstrated widespread substrate tolerance, which can photocatalytically oxidize various alcohols to afford corresponding aldehydes under the identical conditions.

The interesting photocatalytic results prompted us to study the photoelectrochemical properties of CZJ-18(Zn)-Cu (Figure 3). The as-synthesized CZJ-18(Zn)-Cu was deposited on fluorine-doped tin oxide (FTO) surface. The photocurrent profile of the photoelectrode indicates that CZJ-18(Zn)-Cu is highly photoactive, which presents evident photo-generated current responses to changes in the light on/off states in the presence of co-catalyst TEMPO. The maximum photo-generated current response value of CZJ-18(Zn)-Cu/FTO electrode is about 23 μA cm^{-2}. The maximum photo-generated current response value is increased to 37 μA cm^{-2} in the presence of 2,2'-bipyridine, which suggests that 2,2'-bipyridine plays important roles to improve the photocatalytic properties of the catalyst platform by tuning the electronic coordination environment of $\mathrm{Cu^{II}}$ ions. In contrast, the photocurrent density of blank FTO electrode is ignorable. These results clearly demonstrated the excellent photocatalytic properties of CZJ-18(Zn)-Cu in aerobic oxidation.

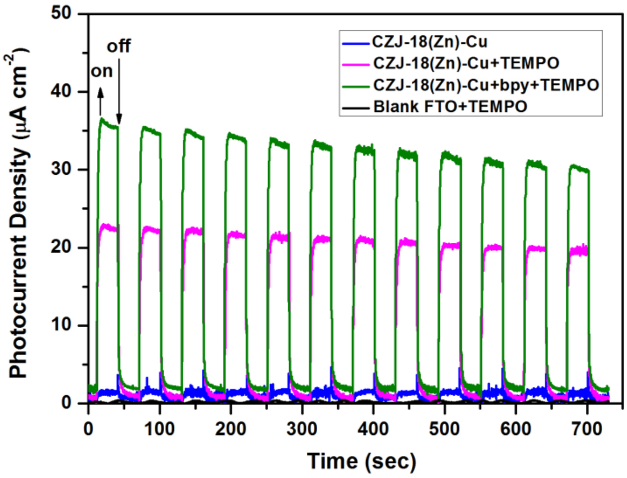

Figure 3. Transient photocurrent responses of CZJ-18(Zn)-Cu in 0.1 M $\mathrm{Bu_4NClO_4}$ acetonitrile solution at a bias of 0 V (vs. SCE electrode) at room temperature under a 300 W Xenon lamp irradiation with a 400 nm light cut-off filter.

Table 1. Asymmetric aldol addition reaction catalyzed by CZJ-18(Cu)-Pro[a].

Entry	Substrates	Yield(%)[b]	Anti:syn[c]	ee(%)[d]
1	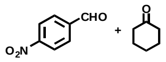	95	5:1	88
2	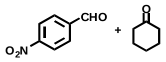	>99	3:2	93[e]
3	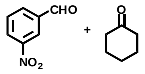	91	2:1	71
4	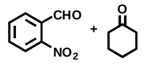	83	3:1	73
5	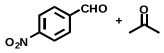	82	-	29
6	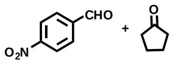	96	1:1	61

[a] Reaction conditions: aldehyde (0.01 mmol), ketone (75 μL), catalyst (1 μmol), HBF_4 (2 μmol), H_2O (25 μL) and DMF (0.2 mL) were stirred at room temperature for 4 days. [b] Isolated yield. [c] Determined by ^1H NMR. [d] Determined by HPLC on a chiral AD-H or AS-H column, and the ee value is for the major anti isomer. [e] Catalyzed by L-proline.

Chiral catalysts consisting of carboxylate groups can also be easily incorporated in CZJ-18(M) for highly efficient asymmetric catalysis. We selected L-proline as a representative of chiral organic catalysts to synthesize chiral catalyst CZJ-18(Cu)-Pro.[30-36] CZJ-18(Cu)-Pro efficiently catalyzed the aldol addition reaction between cyclohexanone and 4-nitrobenzaldehyde, affording the corresponding products in 95% total yield with anti to syn diastereomeric ratio (dr) of 5:1 and 88% ee for the anti isomer (Table 1). In contrast, molecular L-proline resulted in low diastereomeric ratio (3:2) with 93% ee for the anti isomer under the same conditions. The improved dr catalyzed by heterogeneous CZJ-18(Cu)-Pro may originate from the restricted movement of the catalytic sites in the nanopore space, the limited accessibility of the active centers to reactant molecules and the confined formation of the cyclic transition states for the aldol addition products. CZJ-18(Cu)-Pro can be reused for five successive runs with almost retained catalytic properties in the asymmetric aldol reaction. CZJ-18(Cu)-Pro is also highly efficient and selective in asymmetric aldol addition reaction between various aldehydes and ketones.

In summary, we report a versatile metalloporphyrinic framework platform, which is systematically tunable with different functional moieties for highly efficient bioinspired catalysis, photocatalysis and asymmetric catalysis. The catalyst platform is significantly superior to the corresponding molecular catalyst systems, because incorporation of different active species in the pore space/matrices would endow them effectively cooperative work. Since a substantial number of functional moieties are readily being incorporated into the robust platform, a library of highly efficient heterogeneous catalysts can be simply created for various catalytic applications.

Acknowledgements

We are grateful for the financial support of the National Natural Science Foundation of China (grant nos. 21373180, 21525312 and 21872122).

Keywords: Suspended ion catalyst • Synergistic work • Bioinspired catalysis • Photocatalysis • Asymmetric catalysis

[1] J. T. Groves, In Cytochrome P450: structure, mechanism, and biochemistry, 3rd ed.; Ortiz de Montellano, P. R. (Ed.) Kluwer Academic/Plenum: New York, **2005**.
[2] T. L. Poulos, *Chem. Rev.* **2014**, *114*, 3919-3962.
[3] C.-D. Wu, M. Zhao, *Adv. Mater.* **2017**, *29*, 1605446.
[4] K. Chen, C.-D. Wu, *Coord. Chem. Rev.* **2018**, *378*, 445-465.
[5] H. Furukawa, K. E. Cordova, M. O'Keeffe, O. M. Yaghi, *Science* **2013**, *341*, 1230444-1230457.
[6] H.-C. Zhou, S. Kitagawa, *Chem. Soc. Rev.* **2014**, *43*, 5415-5418.
[7] G. Maurin, C. Serre, A. Cooper, G. Férey, *Chem. Soc. Rev.* **2017**, *46*, 3104-3107.
[8] T. Islamoglu, S. Goswami, Z. Li, A. J. Howarth, O. K. Farha, J. T. Hupp, *Acc. Chem. Res.* **2017**, *50*, 805-813.
[9] B. Li, H.-M. Wen, Y. Cui, W. Zhou, G. Qian, B. Chen, *Adv. Mater.* **2016**, *28*, 8819-8860.
[10] W. P. Lustig, S. Mukherjee, N. D. Rudd, A. V. Desai, J. Li, S. K. Ghosh, *Chem. Soc. Rev.* **2017**, *46*, 3242-3285.
[11] Q.-L. Zhu, Q. Xu, *Chem. Soc. Rev.* **2014**, *43*, 5468-5512.
[12] Q.-G. Zhai, X. Bu, X. Zhao, D.-S. Li, P. Feng, *Acc. Chem. Res.* **2017**, *50*, 407-417.
[13] L. Jiao, Y. Wang, H.-L. Jiang, Q. Xu, *Adv. Mater.* **2017**, *30*, 1703663.
[14] A. H. Chughtai, N. Ahmad, H. A. Younus, A. Laypkov, F. Verpoort, *Chem. Soc. Rev.* **2015**, *44*, 6804-6849.
[15] M. Yoon, R. Srirambalaji, K. Kim, *Chem. Rev.* **2012**, *112*, 1196-1231.
[16] H. R. Moon, D.-W. Lim, M. P. Suh, *Chem. Soc. Rev.* **2013**, *42*, 1807-1824.
[17] A. Dhakshinamoorthy, H. Garcia, *Chem. Soc. Rev.* **2014**, *43*, 5750-5765.
[18] T. Zhang, W. Lin, *Chem. Soc. Rev.* **2014**, *43*, 5982-5993.
[19] J. Liu, L. Chen, H. Cui, J. Zhang, L. Zhang, C.-Y. Su, *Chem. Soc. Rev.* **2014**, *43*, 6011-6061.
[20] Y. Wen, J. Zhang, Q. Xu, X.-T. Wu, Q.-L. Zhu, *Coord. Chem. Rev.* **2018**, *376*, 248-276.
[21] W. Y. Gao, M. Chrzanowski, S. Ma, *Chem. Soc. Rev.* **2014**, *43*, 5841-5866.
[22] X. Lian, Y. Fang, E. Joseph, Q. Wang, J. Li, S. Banerjee, C. Lollar, X. Wang, H.-C. Zhou, *Chem. Soc. Rev.* **2017**, *46*, 3386-3401.
[23] M. Zhao, S. Ou, C.-D. Wu, *Acc. Chem. Res.* **2014**, *47*, 1199-1207.
[24] W.-L. He, X.-L. Yang, M. Zhao, C.-D. Wu, *J. Catal.* **2018**, *358*, 43-49.
[25] C. D. Wagner, W. M. Riggs, L. E. Davis, J. F. Moulder, G. E. Muilenberg, (Eds.) Handbook of X-ray photoelectron spectroscopy, Perkin-Elmer Corporation Physical Electronics Division, Minnesota, **1979**.
[26] M. S. Holzwarth, B. Plietker, *ChemCatChem* **2013**, *5*, 1650-1679.
[27] B. L. Ryland, S. S. Stahl, *Angew. Chem. Int. Ed.* **2014**, *53*, 8824-8838.
[28] J. A. Johnson, X. Zhang, T. C. Reeson, Y.-S. Chen, J. Zhang, *J. Am. Chem. Soc.* **2014**, *136*, 15881-15884.
[29] C. Wang, K. E. deKraft, W. Lin, *J. Am. Chem. Soc.* **2012**, *134*, 7211-7214.
[30] S. Mukherjee, J. W. Yang, S. Hoffmann, B. List, *Chem. Rev.* **2007**, *107*, 5471-5569.
[31] P. Kumar, N. Dwivedi, *Acc. Chem. Res.* **2013**, *46*, 289-299.
[32] D. J. Lun, G. I. N. Waterhouse, S. G. Telfer, *J. Am. Chem. Soc.* **2011**, *133*, 5806-5809.
[33] D. Dang, P. Wu, C. He, Z. Xie, C. Duan, *J. Am. Chem. Soc.* **2010**, *132*, 14321-14323.
[34] C. Zhu, Q. Xia, X. Chen, Y. Liu, X. Du, Y. Cui, *ACS Catal.* **2016**, *6*, 7590-7596.
[35] J. Bonnefoy, A. Legrand, E. A. Quadrelli, J. Canivet, D. Farrusseng, *J. Am. Chem. Soc.* **2015**, *137*, 9409-9416.
[36] C. Kutzscher, G. Nickerl, I. Senkovska, V. Bon, S. Kaskel, *Chem. Mater.* **2016**, *28*, 2573-2580.

Entry for the Table of Contents

COMMUNICATION

The functionalities of a metalloporphyrinic framework platform are systematically tunable for highly efficient bioinspired catalysis, photocatalysis and asymmetric catalysis. This work demonstrates that incorporation of different active species in the pore space/matrices of the platform would endow them effectively cooperative catalysis.

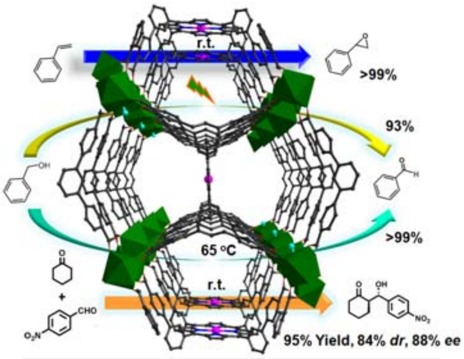

*Wei-Long He, Min Zhao, and Chuan-De Wu**

Page No. – Page No.

A Versatile Metalloporphyrinic Framework Platform for Highly Efficient Bioinspired, Photo and Asymmetric Catalysis